

Fig. 1S. FTIR spectra of raw PS, TEPA-PS, TETA-PS and DETA-PS (A) and DR80 adsorption onto TEPA-PS, TETA-PS and DETA-PS (B) at the optimal conditions.

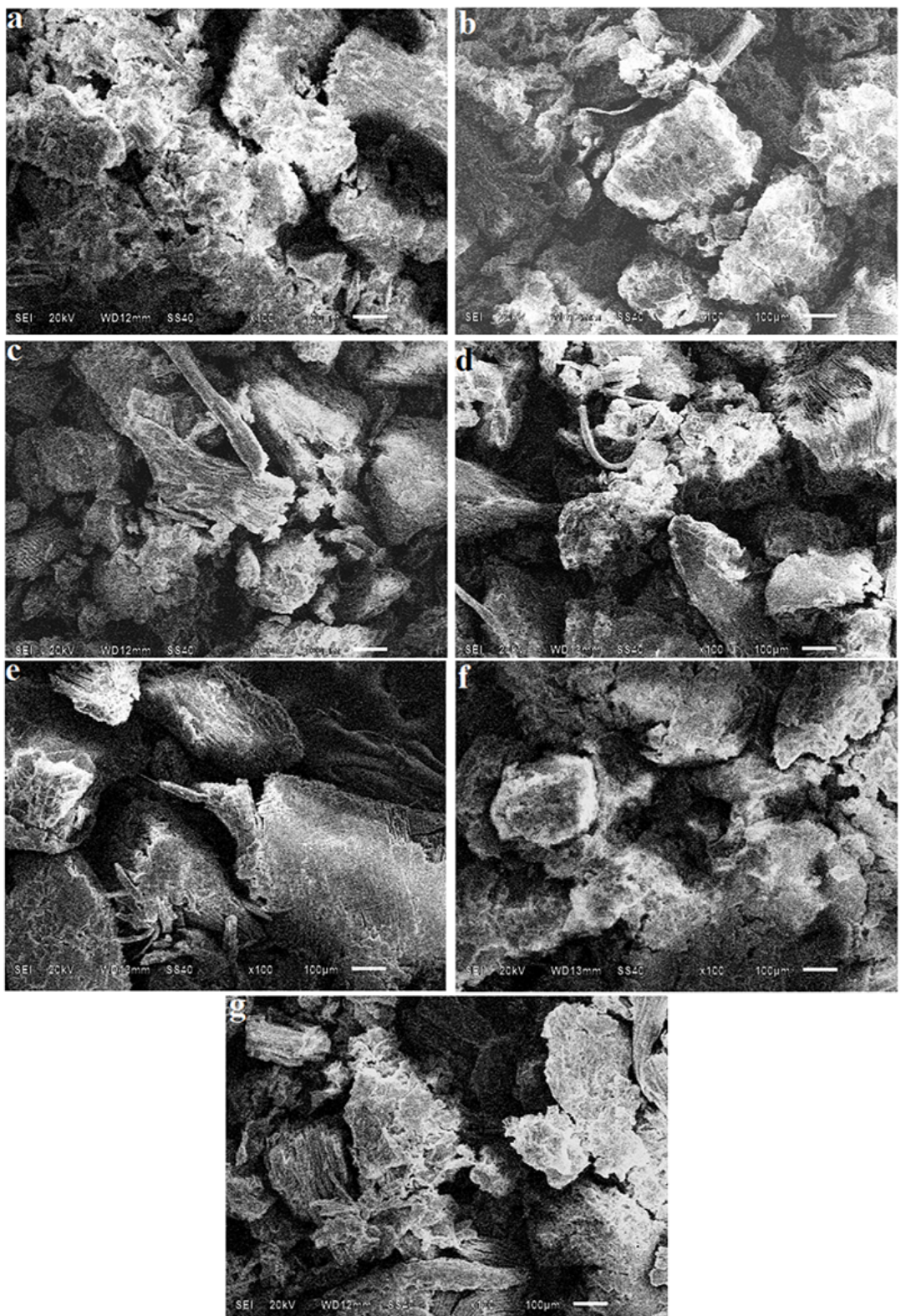


Fig. 2S. Scanning electron micrographs (SEM) of raw PS (a), TEPA-PS (b), TETA-PS (c), DETA-PS (d), TEPA-PS adsorbing DR80 (e), TETA-PS adsorbing DR80 (f), and DETA-PS adsorbing DR80 (g).

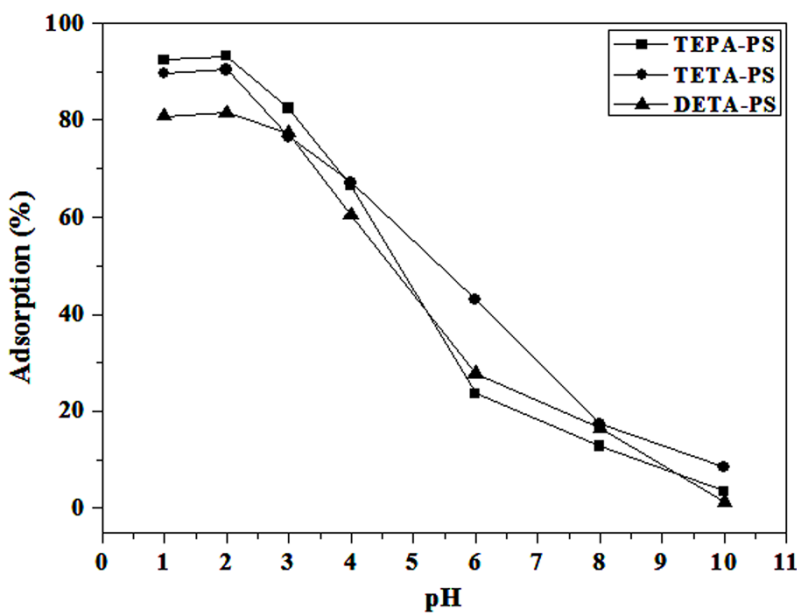


Fig. 3S The effects of pH for DR80 adsorption onto TEPA-PS, TETA-PS, or DETA-PS (initial concentration of DR80 = 140 mg/L, adsorbent dose = 20.0 mg/100mL, $T = 70^\circ\text{C}$ and $t = 180\text{min}$ for the DR80 system).

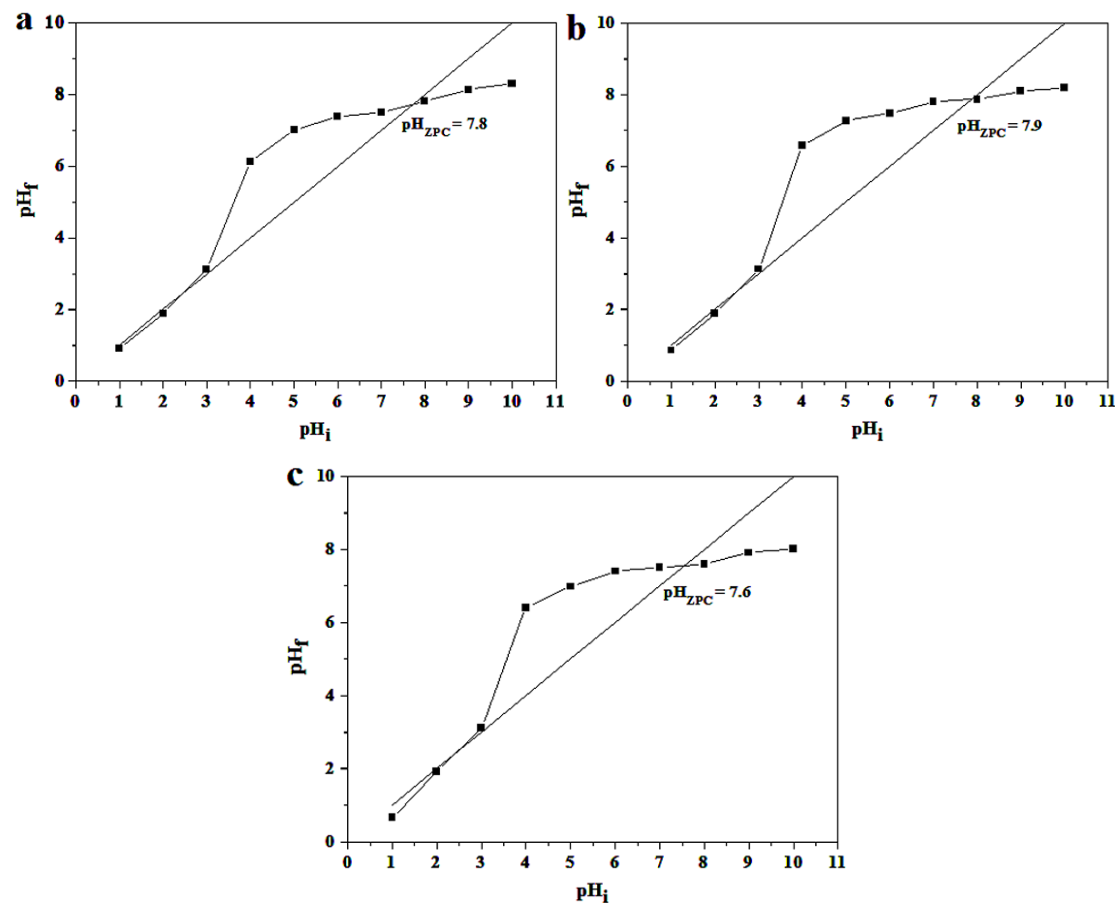


Fig. 4S Determination of the point of zero charge of TEPA-PS (a), TETA-PS (b), and DETA-PS (c).

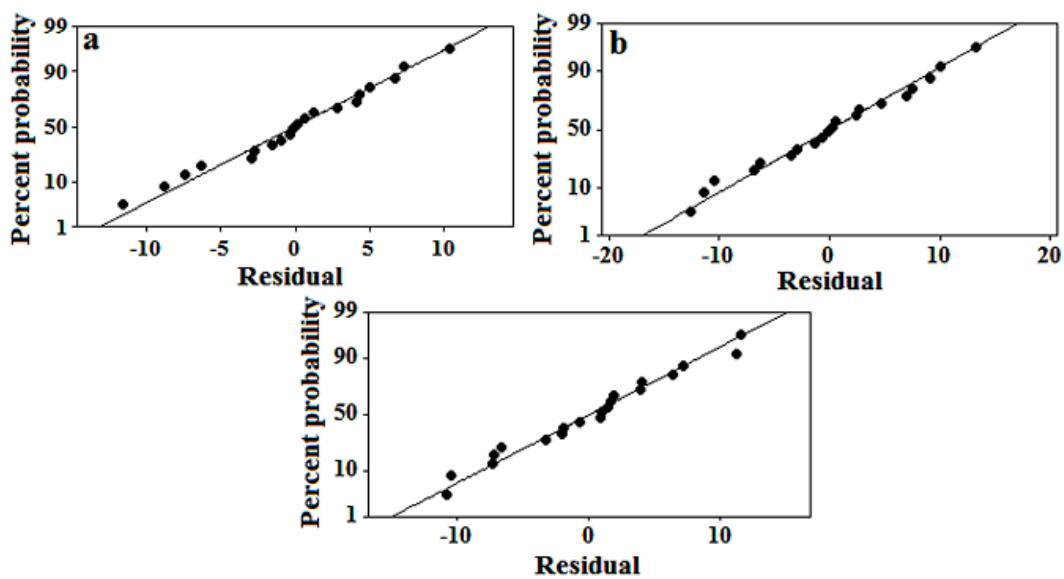
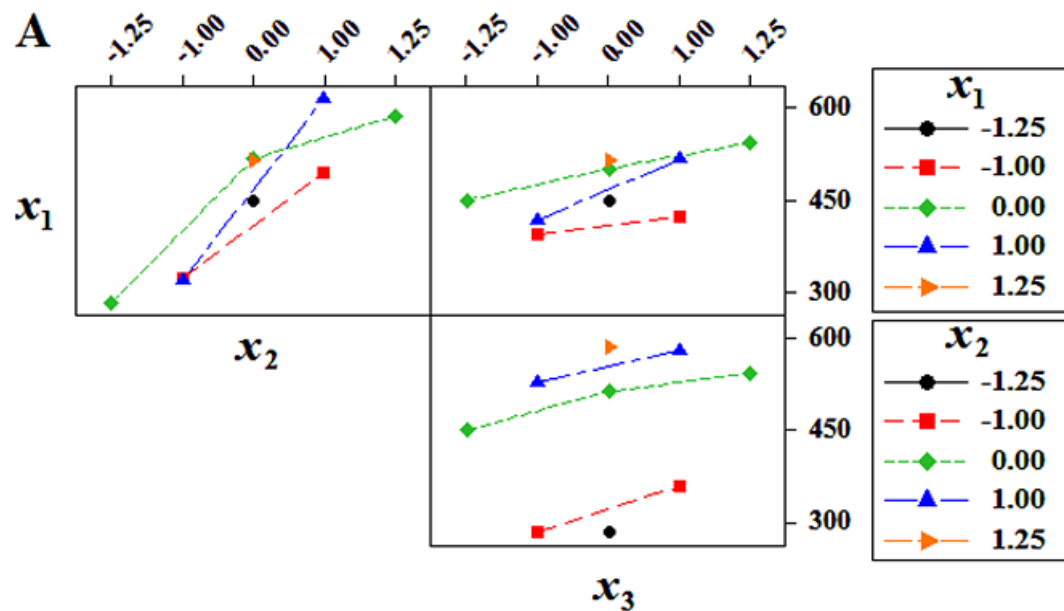


Fig. 5S. Normal probability plots of residuals for the adsorption capacities of DR80 onto TEPA-PS (a), TETA-PS (b), or DETA-PS (c).



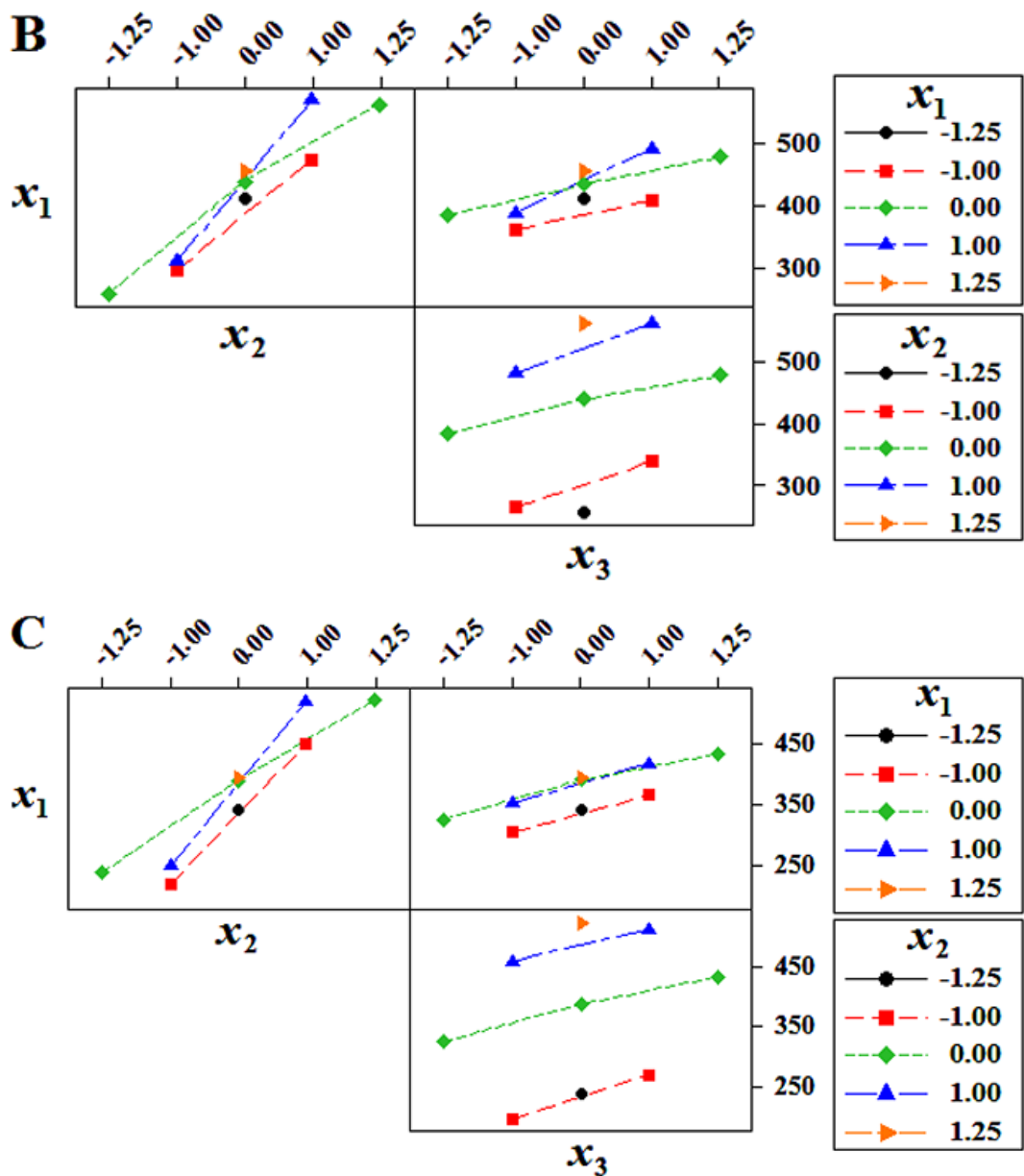


Fig.6S. Interaction effect plots for DR80 removal by TEPA-PS (A), TETA-PS (B), or DETA-PS (C) biosorbent.

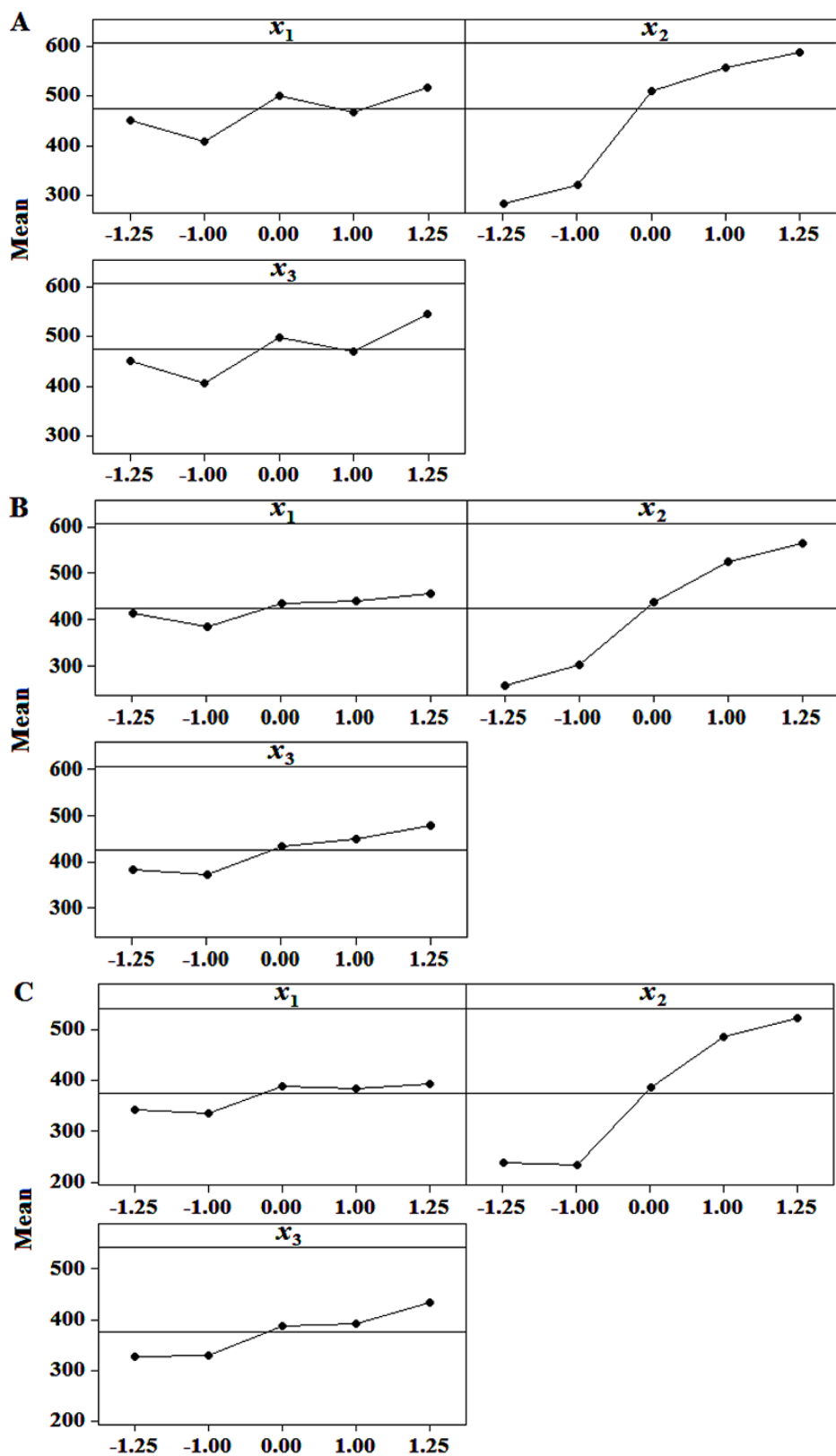


Fig.7S. Main effect plots for DR80 removal by TEPA-PS (A), TETA-PS (B), or DETA-PS (C) biosorbent.

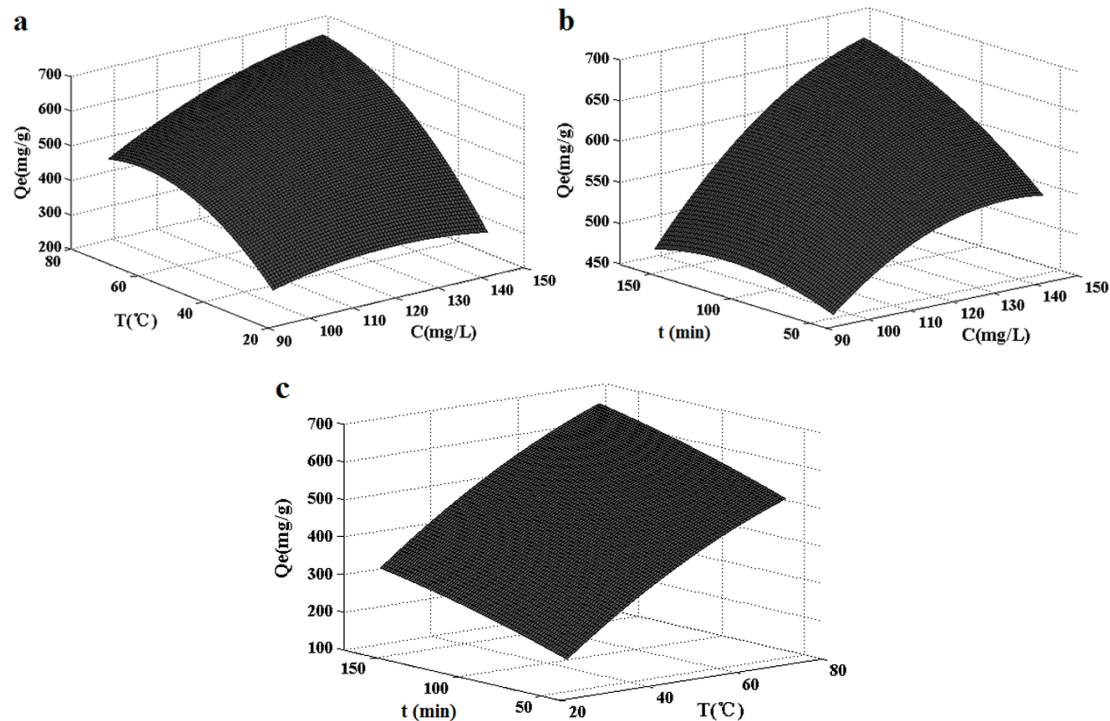


Fig. 8S. Response surface plots of the combined effects for DR80 removal by TEPA-PS: (a) initial concentration of DR80 (C) and temperature of adsorption reaction (T), $t = 150$ min; (b) C and the time of adsorption reaction (t), $T = 70$ °C; (c) T and t , $C = 140$ mg/L.

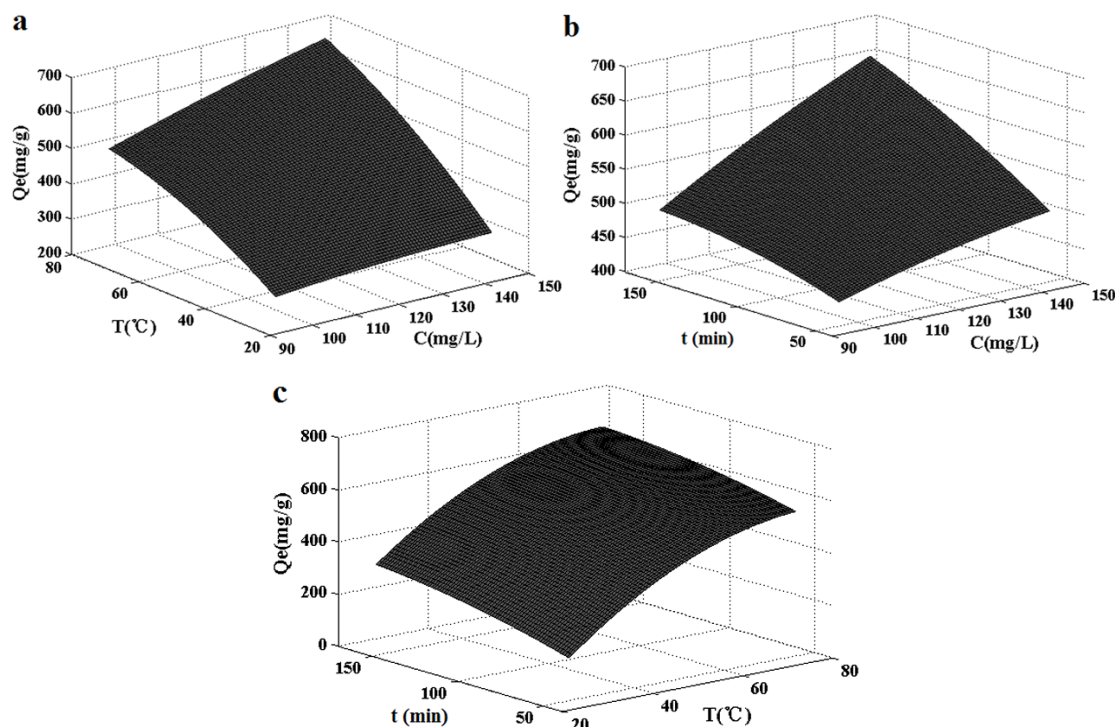


Fig. 9S. Response surface plots of the combined effects for DR80 removal by TETA-PS: (a) initial concentration of DR80 (C) and temperature of adsorption reaction (T), $t = 150$ min; (b) C and the time of adsorption reaction (t), $T = 70$ °C; (c) T and t , $C = 140$ mg/L.

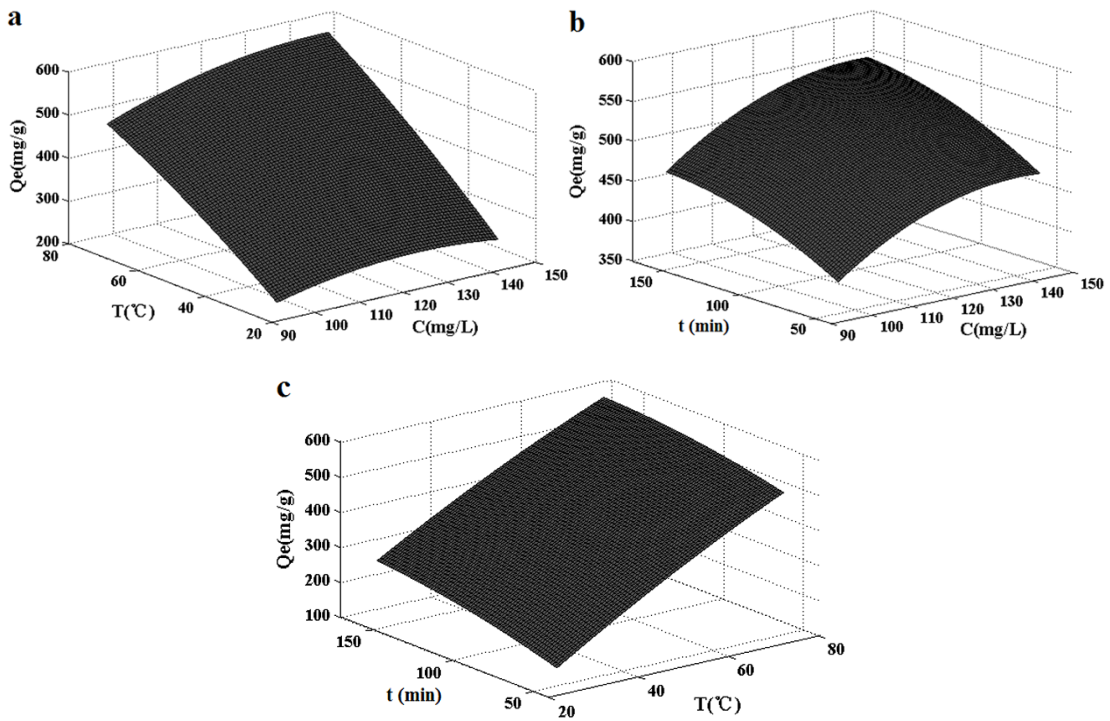
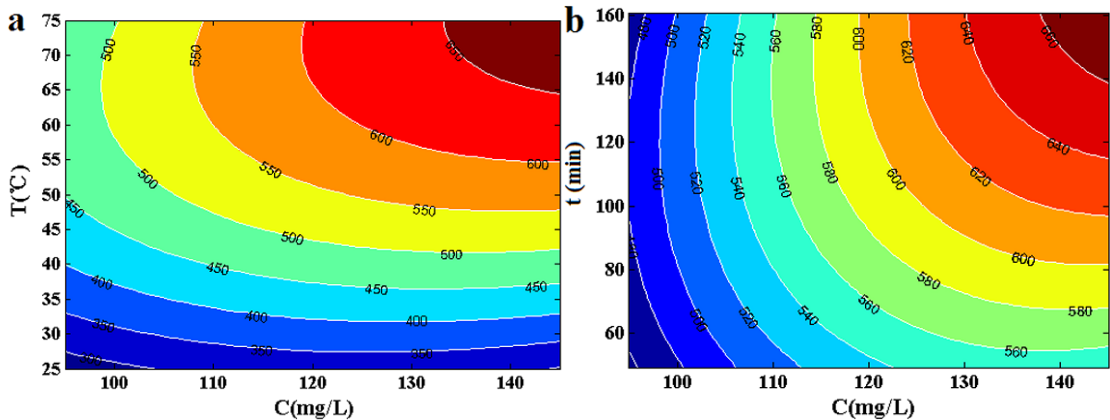


Fig. 10S. Response surface plots of the combined effects for DR80 removal by DETA-PS: (a) initial concentration of DR80 (C) and temperature of adsorption reaction (T), $t = 150\text{min}$; (b) C and the time of adsorption reaction (t), $T = 70^\circ\text{C}$; (c) T and t , $C = 140 \text{ mg/L}$.



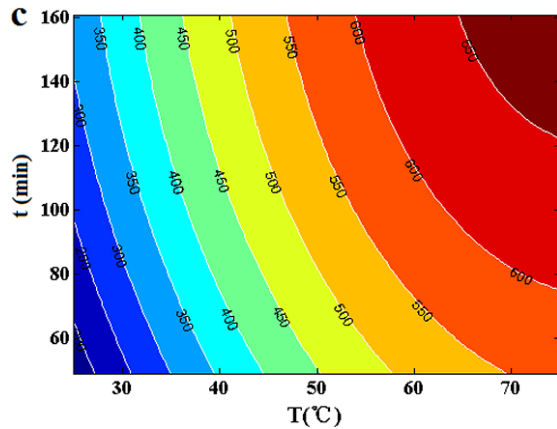


Fig. 11S. Contour plots of the combined effects for DR80 removal by TEPA-PS: (a) initial concentration of DR80 (C) and temperature of adsorption reaction (T), $t = 150\text{min}$; (b) C and the time of adsorption reaction (t), $T = 70^\circ\text{C}$; (c) T and t , $C = 140 \text{ mg/L}$.

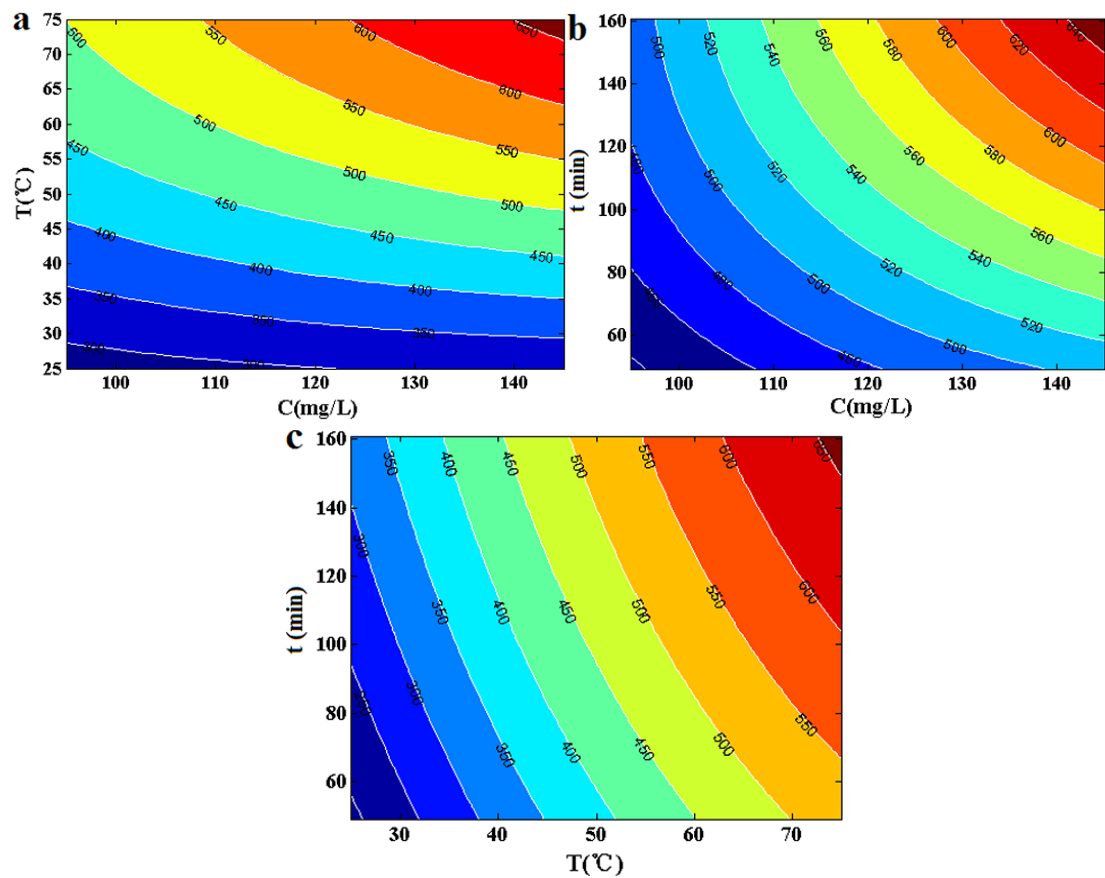


Fig. 12S. Contour plots of the combined effects for DR80 removal by TETA-PS: (a) initial concentration of DR80 (C) and temperature of adsorption reaction (T), $t = 150\text{min}$; (b) C and the time of adsorption reaction (t), $T = 70^\circ\text{C}$; (c) T and t , $C = 140 \text{ mg/L}$.

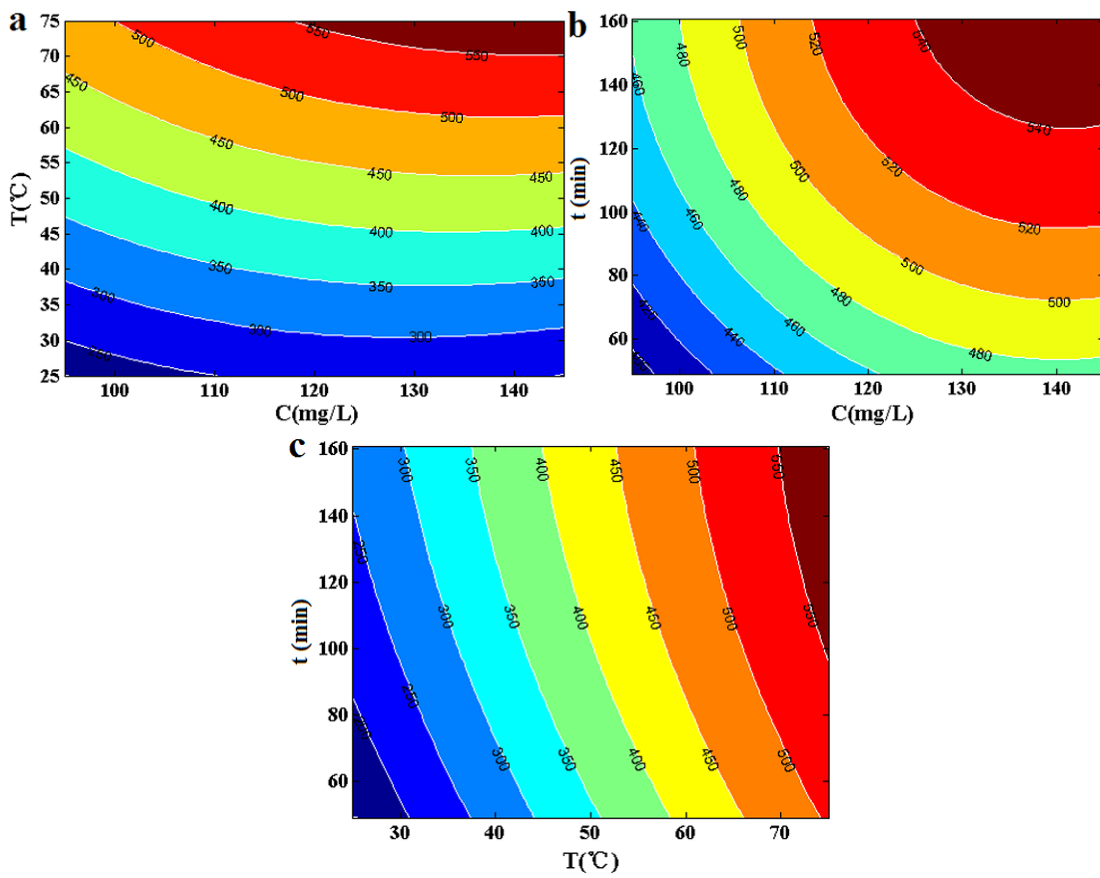
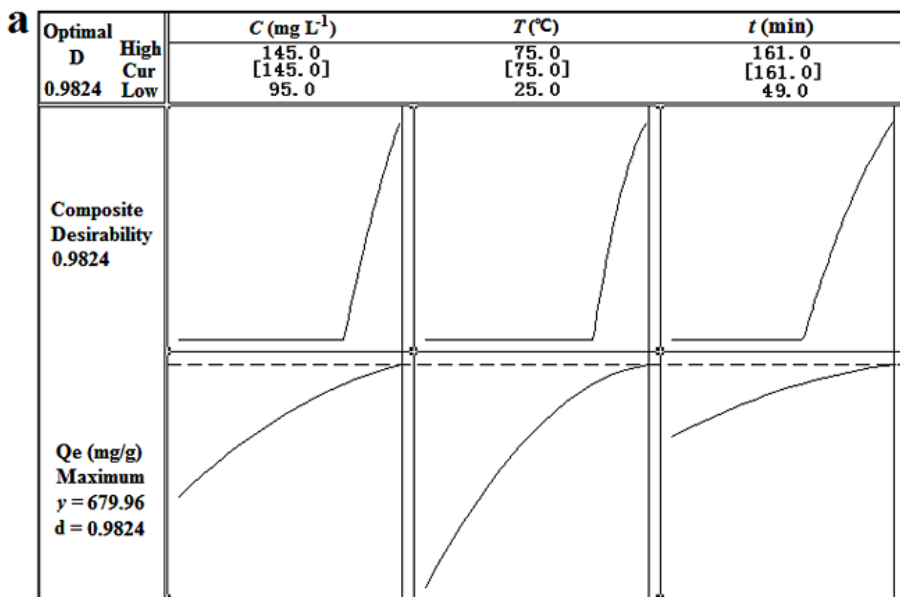


Fig. 13S. Contour plots of the combined effects for DR80 removal by DETA-PS: (a) initial concentration of DR80 (C) and temperature of adsorption reaction (T), $t = 150\text{min}$; (b) C and the time of adsorption reaction (t), $T = 70^\circ\text{C}$; (c) T and t , $C = 140 \text{ mg/L}$.



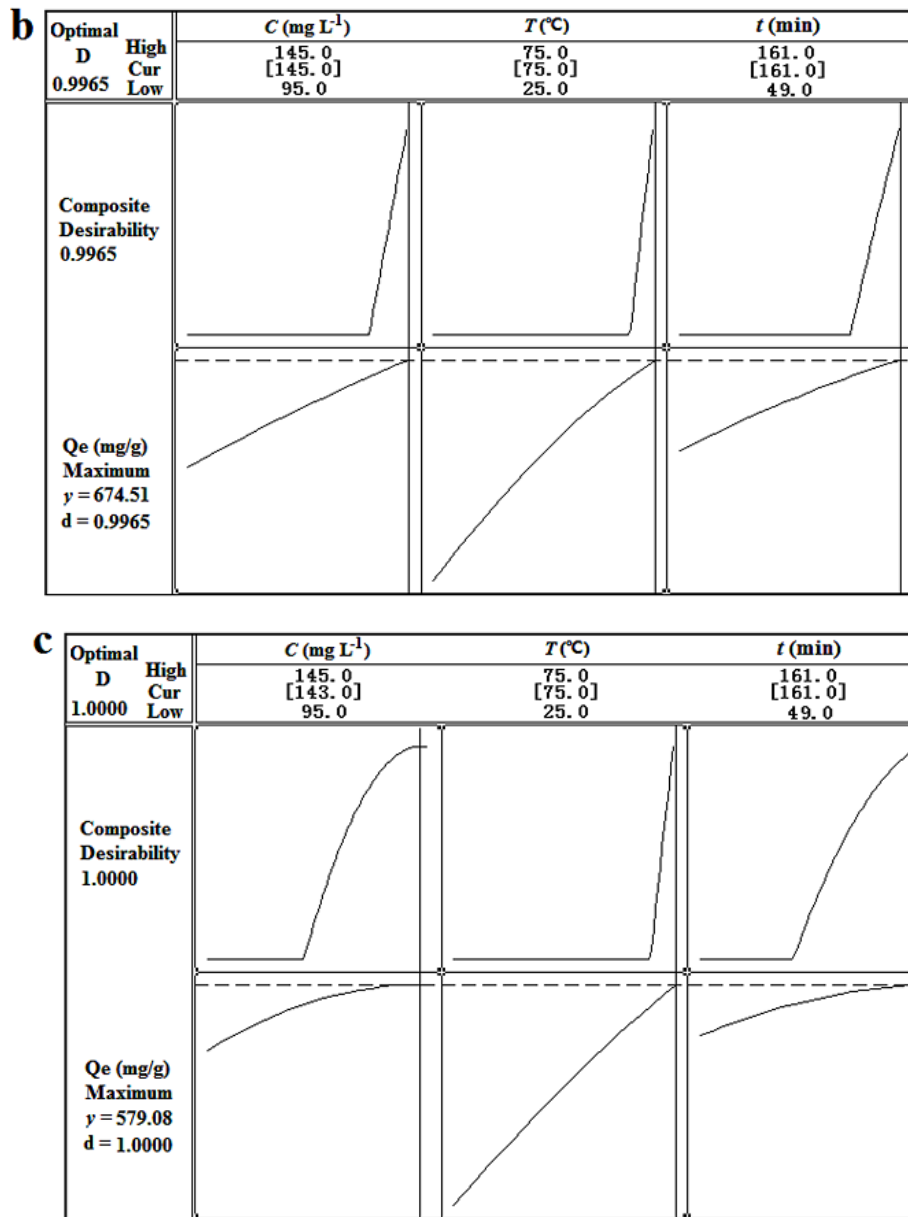


Fig. 14S. Optimization plots for DR80 adsorption by TEPA-PS (a), TETA-PS (b), or DETA-PS (c) biosorbent.

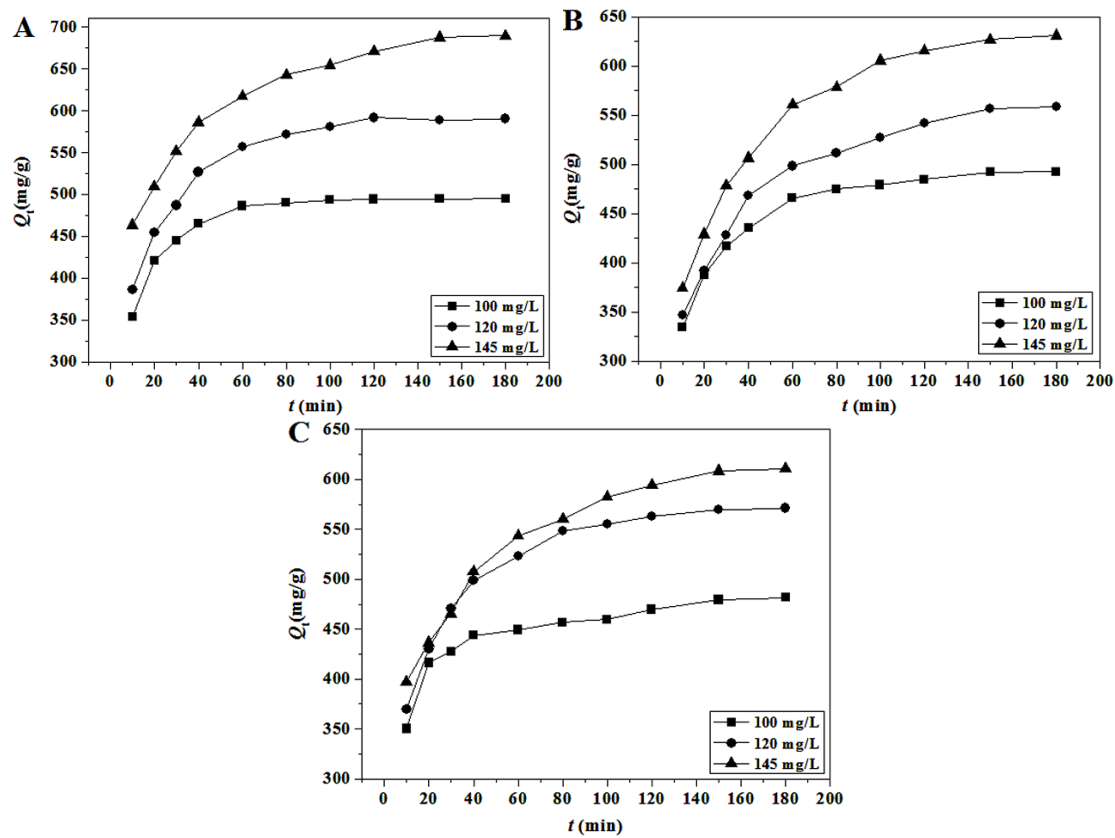
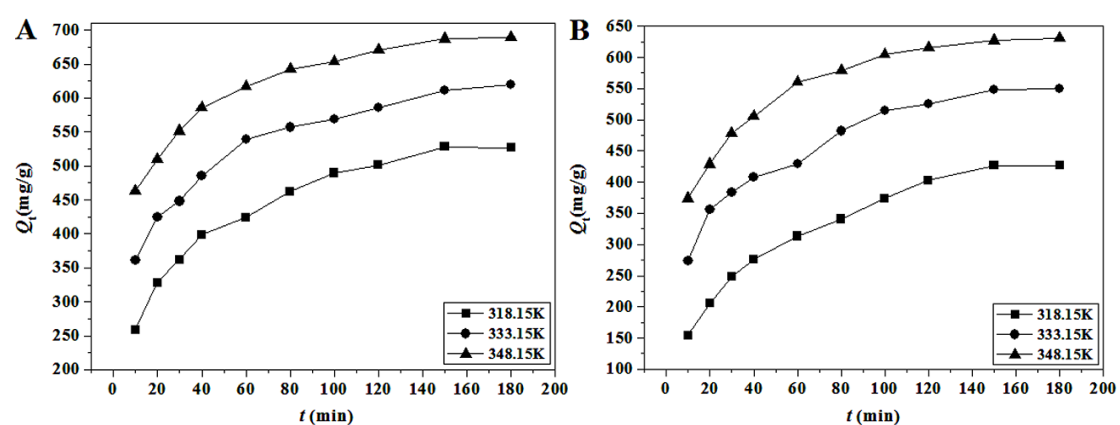


Fig. 15S. The adsorption capacities of DR80 onto TEPA-PS (A), TETA-PS (B) and DETA-PS (C) versus time at different initial concentrations of the dye (adsorbent dose = 20.0 mg/100mL, pH = 2.0, and $T = 75^{\circ}\text{C}$), respectively.



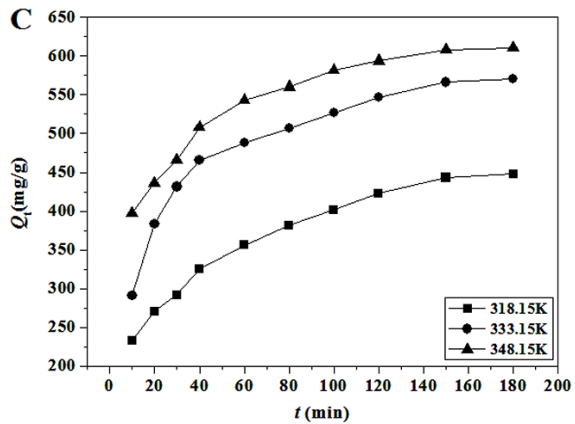


Fig. 16S. The adsorption capacities of DR80 onto TEPA-PS (A), TETA-PS (B) and DETA-PS (C) versus time at different temperatures (adsorbent dose = 20.0 mg/100mL, pH = 2.0, and $C_{DR80} = 145\text{mg/L}$), respectively.

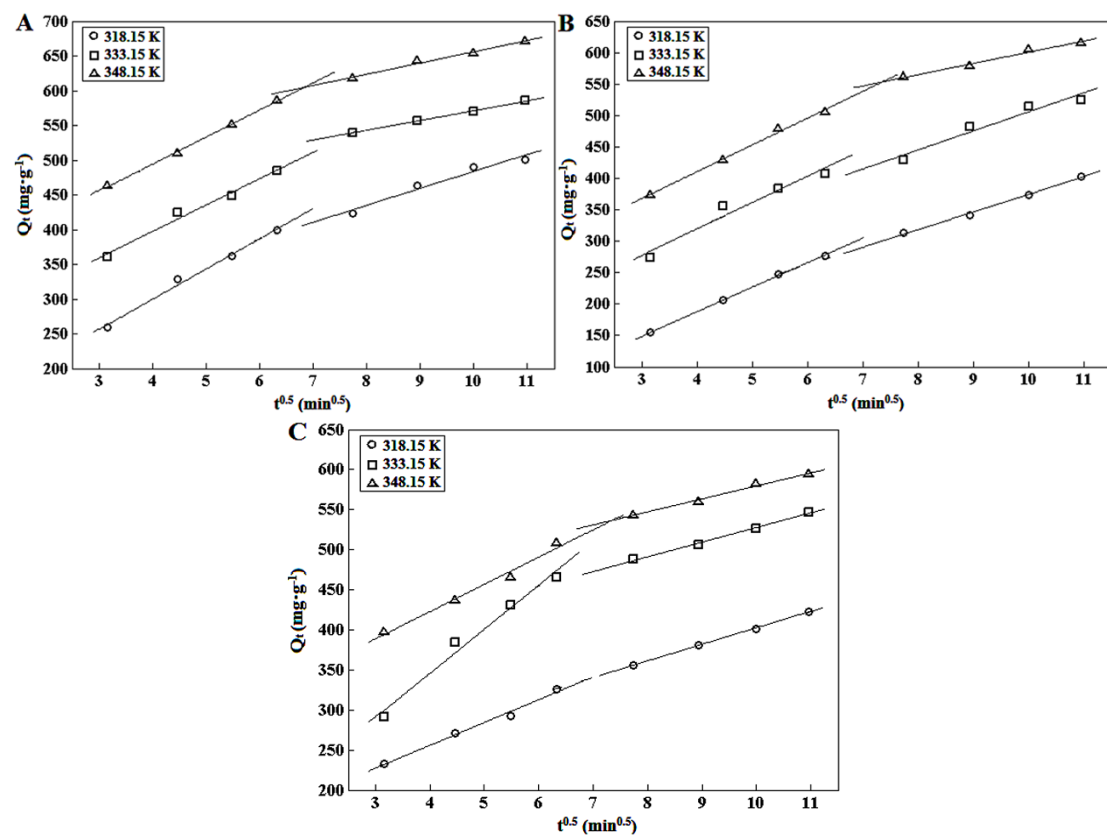


Fig. 17S. Intraparticle diffusion model for DR80 by TEPA-PS (A), TETA-PS (B), or DETA-PS (C) at different temperatures ($C_{DR80} = 145\text{mg/L}$, pH = 2.0, agitation speed = 180 rpm).

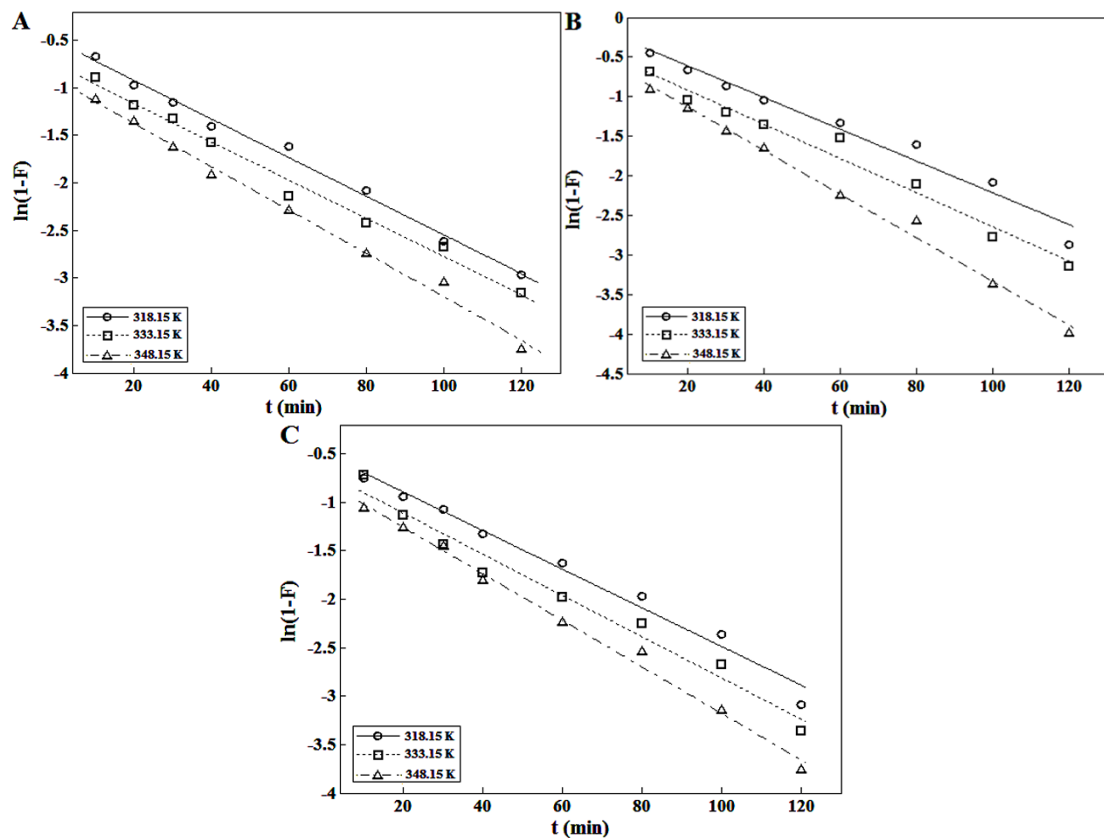
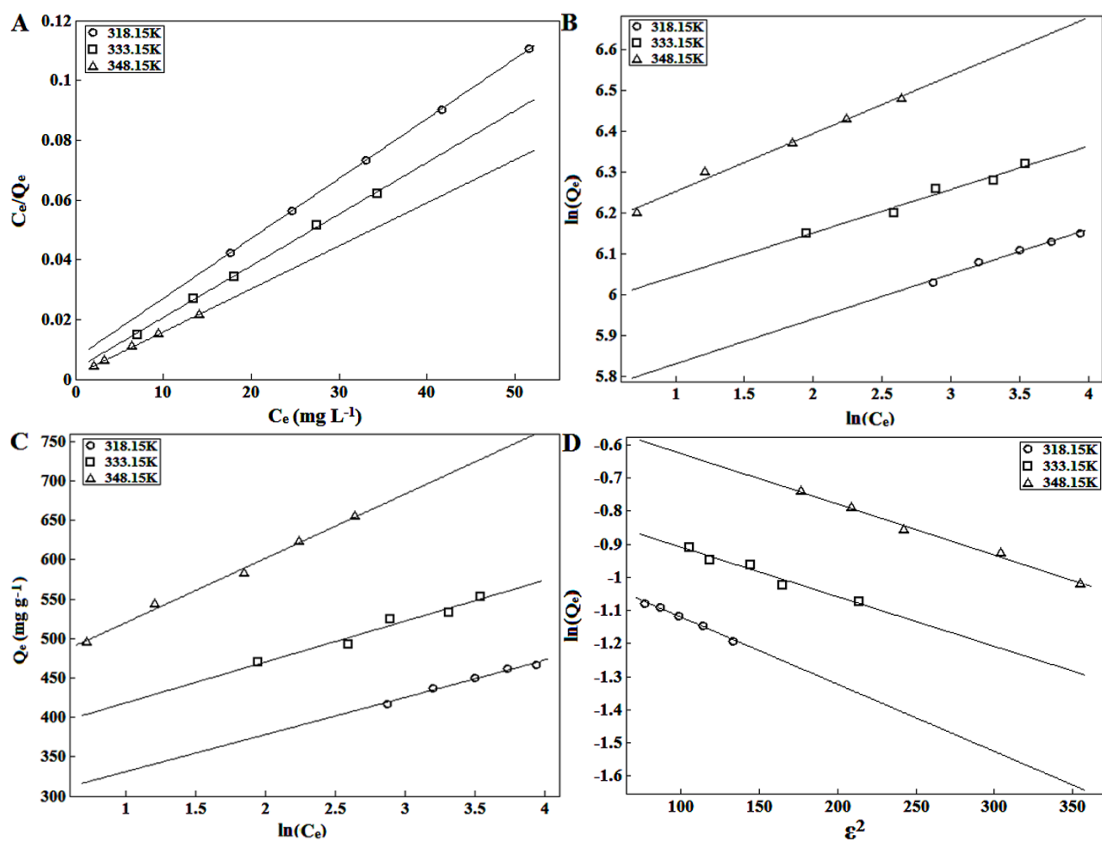


Fig. 18S. Liquid film diffusion model for DR80 by TEPA-PS (A), TETA-PS (B), or DETA-PS (C) at different temperatures ($C_{\text{DR80}} = 145 \text{ mg/L}$, pH = 2.0, agitation speed = 180 rpm).



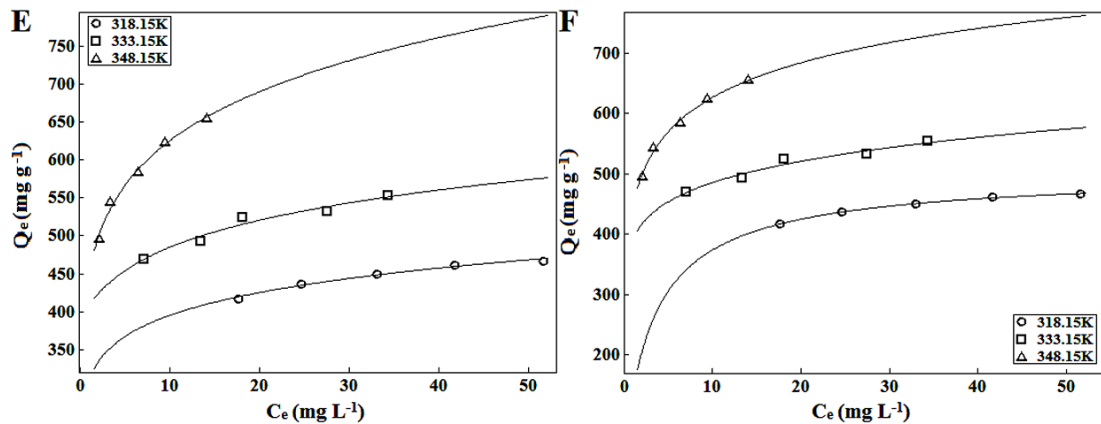
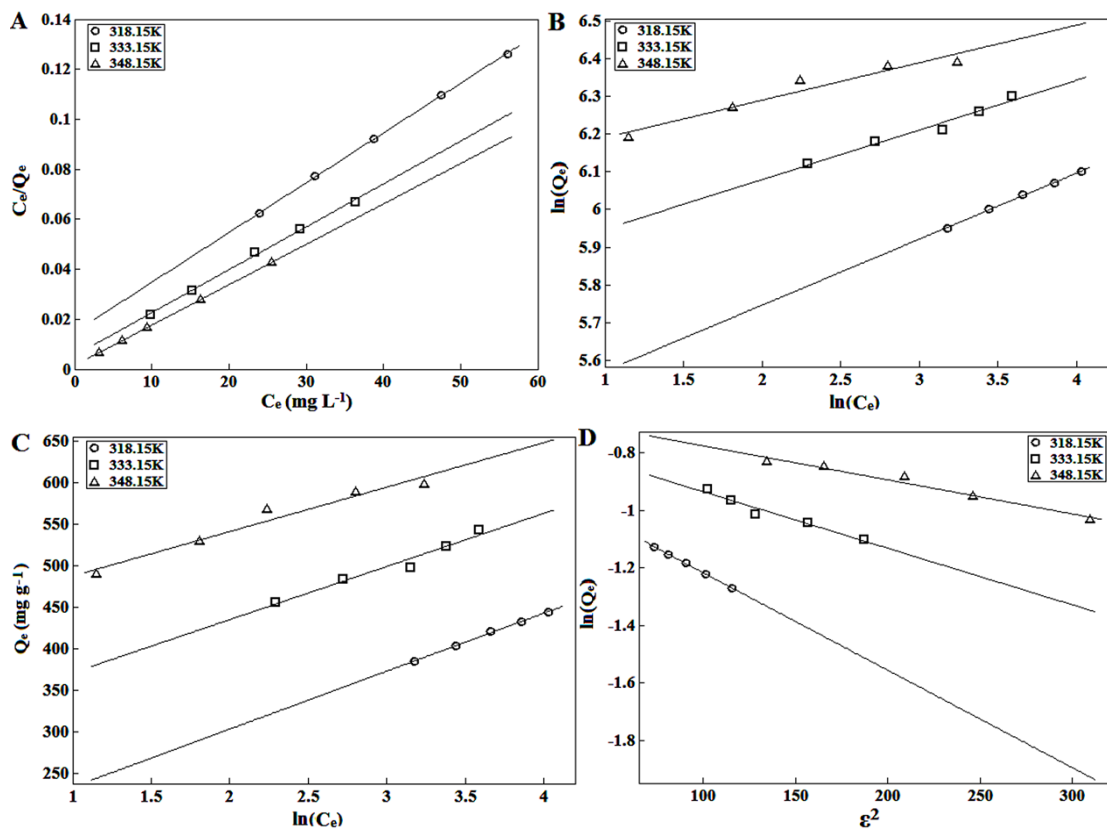


Fig.19S. Adsorption isotherms of DR80 onto TETA-PS using Langmuir (A), Freundlich (B), Temkin (C), Dubinin-Radushkevich (D), Redlich-Peterson (E) or Sips (F) models at different temperatures (adsorbent dose = 20.0 mg/100mL, pH = 2.0, $T = 75^\circ\text{C}$, $t = 161\text{min}$, agitation speed = 180 rpm).



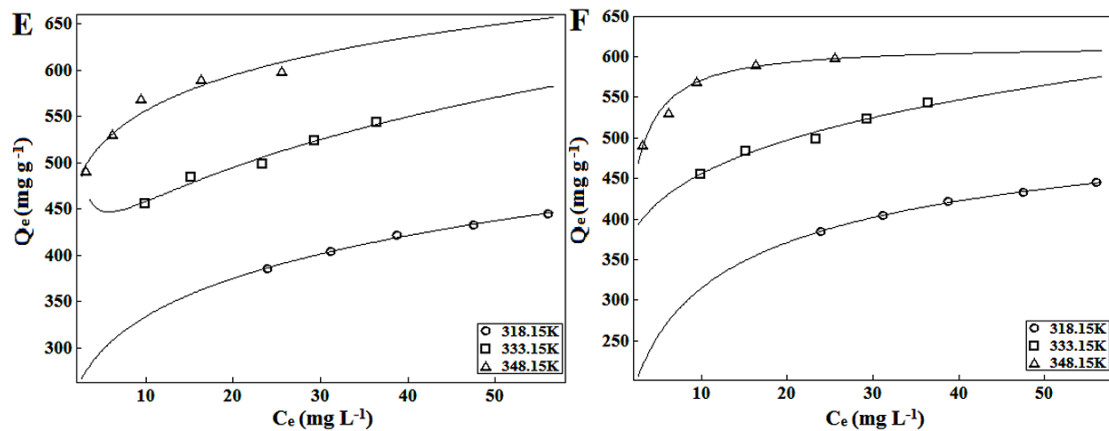


Fig.20S. Adsorption isotherms of DR80 onto DETA-PS using Langmuir (A), Freundlich (B), Temkin (C), Dubinin-Radushkevich (D), Redlich-Peterson (E), or Sips (F) models at different temperatures (adsorbent dose = 20.0 mg/100mL, pH = 2.0, $T = 75^{\circ}\text{C}$, $t = 161\text{min}$, agitation speed = 180 rpm).

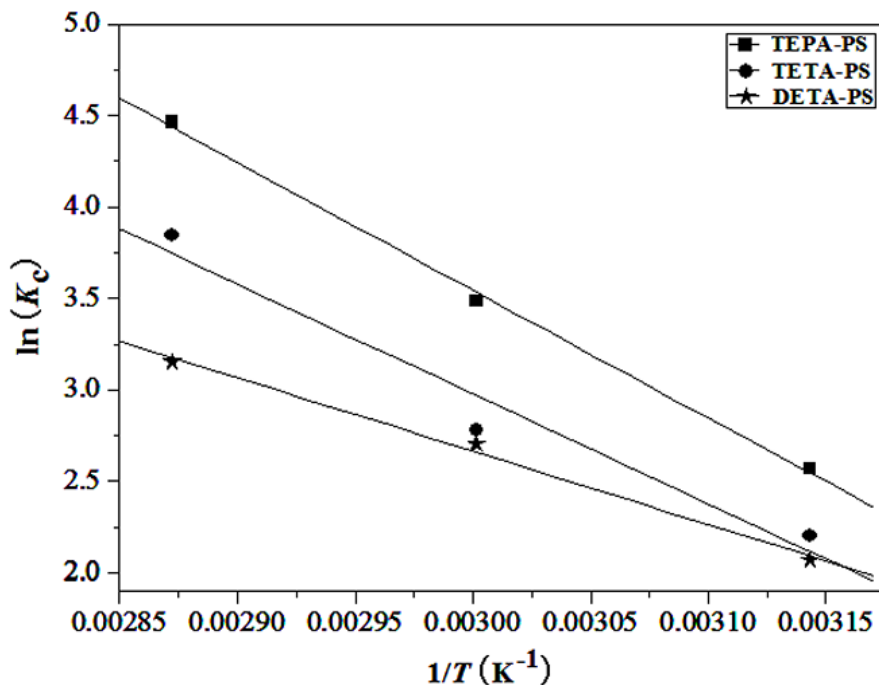


Fig. 21S. Van't Hoff plots for DR80 adsorption on TEPA-PS (■), TETA-PS (●), or DETA-PS (★) (initial concentration of DR80 = 145mg/L, adsorbent dosage = 20.0mg/100mL, pH = 2.0, $T = 75^{\circ}\text{C}$, $t = 161\text{min}$).

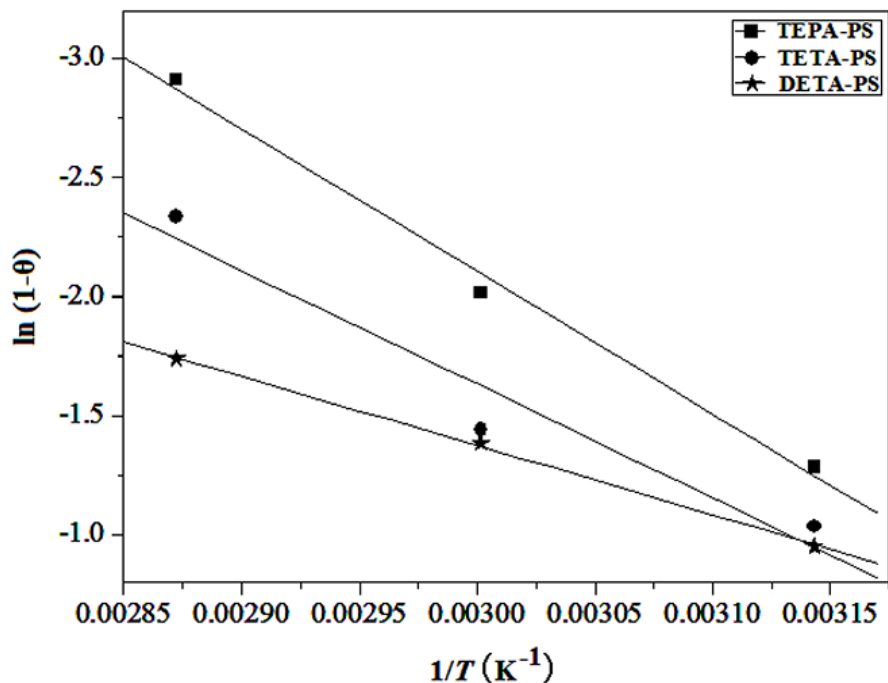


Fig. 22S. Plots of $\ln(1-\theta)$ vs. $1/T$.

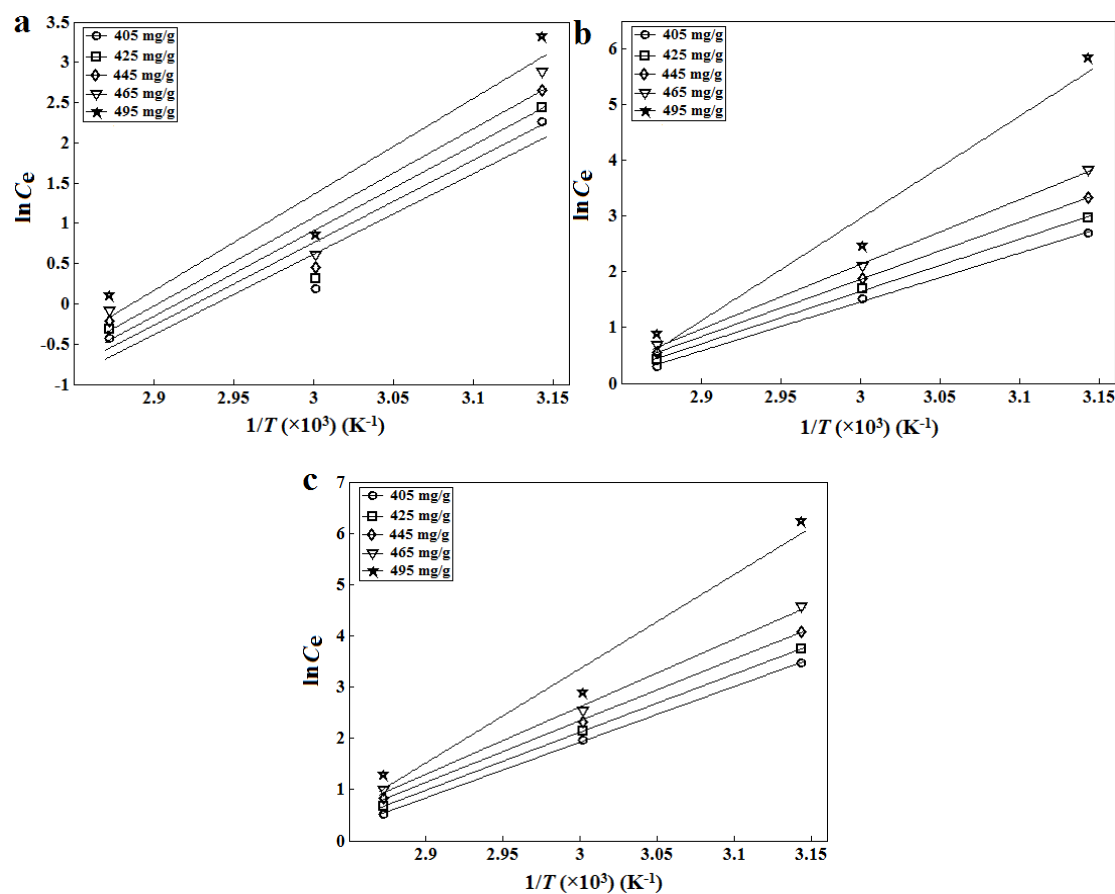


Fig. 23S. Adsorption isosteres for determining isosteric heat of DR80 adsorption onto TEPA-PS (a), TETA-PS (b), or DETA-PS (c). Q_e : 405 mg/g (\circ); 425 mg/g (\square); 445 mg/g (\diamond); 465 mg/g (∇); 495 mg/g (\star).

495mg/g (★).

Table 1S Statistical parameters of central composite design for the TEPA-PS, TETA-PS and DETA-PS systems.

		Term									
system	parameter	Constant	x_1	x_2	x_3	x_1^2	x_2^2	x_3^2	$x_1 x_2$	$x_1 x_3$	$x_2 x_3$
TEPA-PS	Coefficient	521.828	28.737	118.690	33.075	-22.010	-51.338	-12.685	30.830	17.825	-5.758
	Sum of squares	-	9187	156721	12170	10359	18118	953	7604	2542	265
	T-value	180.20	12.38	51.14	14.25	-6.92	-16.14	-3.99	11.27	6.51	-2.10
TETA-PS	PC*	-	4.22	71.92	5.58	4.75	8.31	0.44	3.49	1.17	0.12
	Coefficient	440.773	24.859	114.541	38.221	-4.168	-19.313	-5.726	21.083	14.415	1.362
	Sum of squares	-	6875	145956	16252	802	2616	194	3556	1662	15
DETA-PS	T-value	117.44	8.27	38.08	12.71	-1.01	-4.69	-1.39	5.94	4.06	0.38
	PC*	-	3.86	82.03	9.13	0.45	1.47	0.11	2.00	0.93	0.01
	Coefficient	394.553	24.309	123.496	35.121	-16.563	-9.049	-8.795	10.555	0.963	-5.215
	Sum of squares	-	6574	169670	13723	3077	745	477	891	7	218
	T-value	118.58	9.12	46.31	13.17	-4.53	-2.48	-2.46	3.36	0.31	-1.66
	PC*	-	3.36	86.84	7.02	1.57	0.38	0.24	0.46	0.00	0.11

$$\square \quad *PC(\%) = \frac{SS}{\sum SS} \times 100$$

Table 2S Analysis of variance (ANOVA) of the three fitted quadratic polynomial models.

Source	Degrees of freedom	Sum of squares	Adj. Sum of squares	Adj. Mean squares	F-value	p-value ($F > F_{0.05}$)	Remarks
TEPA-PS							
Regression	9	217919	217919	24213	404	0.000	Significant
x_1	1	9187	9187	9187	153.3	0.000	Significant
x_2	1	156721	156721	156721	2615.7	0.000	Significant
x_3	1	12170	12170	12170	203.1	0.000	Significant
x_1^2	1	10359	2869	2869	47.9	0.000	Significant
x_2^2	1	18118	15610	15610	260.5	0.000	Significant
x_3^2	1	953	953	953	15.9	0.003	Significant
$x_1 x_2$	1	7604	7604	7604	126.9	0.000	Significant
$x_1 x_3$	1	2542	2542	2542	42.4	0.000	Significant
$x_2 x_3$	1	265	265	265	4.4	0.062	
Residual error	10	599	599	59.9			
Lack of fit	5	556	556	111.2	12.87	0.007	Significant
Pure error	5	43	43	8.6			
Total	19	218518					
TETA-PS							
Regression	9	177928	177928	19770	196	0.000	Significant
x_1	1	6875	6875	6875	68.3	0.000	Significant
x_2	1	145956	145956	145956	1450.3	0.000	Significant
x_3	1	16252	16252	16252	161.5	0.000	Significant
x_1^2	1	802	103	103	1.02	0.336	
x_2^2	1	2616	2209	2209	22.0	0.001	Significant
x_3^2	1	194	194	194	1.93	0.195	
$x_1 x_2$	1	3556	3556	3556	35.3	0.000	Significant
$x_1 x_3$	1	1662	1662	1662	16.5	0.002	Significant
$x_2 x_3$	1	15	15	15	0.15	0.709	
Residual error	10	1006	1006	100.6			
Lack of fit	5	950	950	190.1	16.99	0.004	Significant
Pure error	5	56	56	11.2			
Total	19	178934					
DETA-PS							
Regression	9	195383	195383	21709	274	0.000	Significant
x_1	1	6574	6574	6574	83.1	0.000	Significant
x_2	1	169670	169670	169670	2145	0.000	Significant
x_3	1	13723	13723	13723	173.5	0.000	Significant
x_1^2	1	3077	1625	1625	20.5	0.001	Significant
x_2^2	1	745	485	485	6.13	0.033	Significant
x_3^2	1	477	477	477	6.03	0.034	Significant
$x_1 x_2$	1	891	891	891	11.27	0.007	Significant
$x_1 x_3$	1	7	7	7	0.09	0.766	
$x_2 x_3$	1	218	218	218	2.75	0.128	
Residual error	10	791	791	79.1			
Lack of fit	5	720	720	143.9	10.09	0.012	Significant

Pure error	5	71	71	14.3
Total	19	196174		

Table 3S Comparison of intraparticle and liquid film diffusion model parameters at three concentration and temperature levels for DR80 removal by different biosorbents.

model	C_0 (mg·L ⁻¹)	parameter						T/K	parameter							
		k_{d1} mg·(g·min ^{0.5}) ⁻¹	k_{d2} mg·(g·min ^{0.5}) ⁻¹	B_1	B_2	R_1	R_2		k_{d1} mg·(g·min ^{0.5}) ⁻¹	k_{d2} mg·(g·min ^{0.5}) ⁻¹	B_1	B_2	R_1	R_2		
TEPA-PS	100	40.22	9.72	230.52	405.86	0.9830	0.9457	318.15	43.58	24.48	125.15	239.12	0.9955	0.9837		
	120	43.53	10.72	252.08	474.43	0.9962	0.9923	333.15	37.97	14.01	245.33	430.97	0.9912	0.9979		
	145	39.04	16.19	337.86	494.08	0.9991	0.9927	348.15	39.04	16.19	337.86	494.08	0.9991	0.9927		
intraparticle diffusion model	100	32.12	5.76	237.24	421.76	0.9911	0.9935	318.15	39.00	28.06	31.65	93.73	0.9993	0.9973		
	TETA-PS	120	37.74	13.65	225.49	391.32	0.9974	0.9973	333.15	41.81	30.29	152.30	202.62	0.9754	0.9729	
	145	42.58	17.85	240.04	422.03	0.9980	0.9899	348.15	42.58	17.85	240.04	422.03	0.9980	0.9899		
DETA-PS	100	28.61	6.00	270.49	402.41	0.9506	0.9731	318.15	28.50	20.72	141.77	195.44	0.9945	0.9996		
	120	40.94	11.96	243.44	434.53	0.9975	0.9609	333.15	55.08	18.36	125.27	344.18	0.9910	0.9979		
	145	34.07	16.20	286.36	417.65	0.9918	0.9958	348.15	34.07	16.20	286.36	417.65	0.9918	0.9958		
		k_{fd}/min^{-1}			intercept		R		k_{fd}/min^{-1}			intercept		R		
TEPA-PS	100	0.0537			-0.7660		0.9962		318.15	0.0203			-0.5164		0.9965	
	120	0.0326			-0.8033		0.9980		333.15	0.0201			-0.7662		0.9945	
	145	0.0228			-0.9207		0.9962		348.15	0.0228			-0.9207		0.9962	
Liquid film diffusion model	100	0.0273			-1.0366		0.9915		318.15	0.0201			-0.2106		0.9840	
	TETA-PS	120	0.0229			-0.7926		0.9940		333.15	0.0216			-0.4895		0.9885
	145	0.0275			-0.5836		0.9960		348.15	0.0275			-0.5836		0.9960	
DETA-PS	100	0.0192			-1.5299		0.9571		318.15	0.0199			-0.4960		0.9908	
	120	0.0294			-0.8201		0.9975		333.15	0.0213			-0.6869		0.9866	
	145	0.0240			-0.7804		0.9965		348.15	0.0240			-0.7804		0.9965	

Table 4S Comparison of the maximum adsorption capacities for DR80 removal onto various adsorbents

adsorbent	Adsorption capacity (mg·g ⁻¹)	refs
Orange peel	21.05, 21.052	1, 2
Egg shell membrane	161.29	3
Soy meal hull	178.57	4
Mixture almond shells	22.422	5
SA/n-TiO ₂	130	6
Polyurethane foam (PUF)	4.50	7
Canola Hull	8.7032	8
Mentha pulegium	52.356	9
PAC	3448	10
SF-CNT	120.48	11
AC/DDAC	526.32	12
TEPA-PS, TETA-PS and DETA-PS	719.42, 694.44 and 617.28	present study

References

- [1] Mokhtar Arami, Nargess Yousefi Limaee, Niyaz Mohammad Mahmoodi, Nooshin Salman Tabrizi, Removal of dyes from colored textile wastewater by orange peel adsorbent: Equilibrium and kinetic studies, *Journal of Colloid and Interface Science* 288 (2005) 371-376.
- [2] F. Doulati Ardejani, Kh. Badii, N. Yousefi Limaee, N.M. Mahmoodi, M. Arami, S.Z. Shafaei, A.R. Mirhabibi, Numerical modelling and laboratory studies on the removal of Direct Red 23 and Direct Red 80 dyes from textile effluents using orange peel, a low-cost adsorbent, *Dyes and Pigments* 73 (2007) 178-185.
- [3] Mokhtar Arami, Nargess Yousefi Limaee, Niyaz Mohammad Mahmoodi, Investigation on the adsorption capability of egg shell membrane towards model textile dyes, *Chemosphere* 65 (2006) 1999-2008.
- [4] Mokhtar Arami, Nargess Yousefi Limaee, Niyaz Mohammad Mahmoodi, Nooshin Salman Tabrizi, Equilibrium and kinetics studies for the adsorption of direct and acid dyes from aqueous solution by soy meal hull, *Journal of Hazardous Materials* B135 (2006) 171-179.
- [5] F. Doulati Ardejani, Kh. Badii, N. Yousefi Limaee, S.Z. Shafaei, A.R. Mirhabibi, Adsorption of Direct Red 80 dye from aqueous solution onto almond shells: Effect of pH, initial concentration and shell type, *Journal of Hazardous Materials* 151 (2008) 730-737.
- [6] Niyaz Mohammad Mahmoodi, Bagher Hayati, Mokhtar Arami, Hajir Bahrami, Preparation, characterization and dye adsorption properties of biocompatible composite (alginate/titania nanoparticle), *Desalination* 275 (2011) 93-101.
- [7] Julieta de Jesus da Silveira Neta, Guilherme Costa Moreira, Carlos Juliano da Silva, César Reis, Efraim Lázaro Reis, Use of polyurethane foams for the removal of the Direct Red 80 and Reactive Blue 21 dyes in aqueous medium, *Desalination* 281 (2011) 55-60.
- [8] Niyaz Mohammad Mahmoodi, Mokhtar Arami, Hajir Bahrami, Shooka Khorramfar, The Effect of pH on the Removal of Anionic Dyes from Colored Textile Wastewater Using a Biosorbent, *Journal of Applied Polymer Science*, 2011, 120, 2996-3003.
- [9] Niyaz Mohammad Mahmoodi, Bagher Hayati, Hajir Bahrami, Mokhtar Arami, Dye Adsorption and Desorption Properties of Mentha pulegium in Single and Binary Systems, *Journal of Applied Polymer Science*, 2011, 122, 1489-1499.
- [10] Niyaz Mohammad Mahmoodi, Farhood Najafi, Abdollah Neshat, Poly (amidoamine-co-acrylic acid) copolymer: Synthesis, characterization and dye removal ability, *Industrial Crops and Products* 42 (2013) 119-125.
- [11] Ghobadi, J.; Arami, M.; Bahrami, H.; Mahmoodi, N. M. Modification of carbon nanotubes with cationic surfactant and its application for removal of direct dyes. *Desalin. Water Treat.* 2013, 1-13.
- [12] Zhengjun Cheng, Lei Zhang, Xiao Guo, Xiaohui Jiang, Tian Li. Adsorption behavior of direct red 80 and congo red onto activated carbon/surfactant: Process optimization, kinetics and equilibrium, *Spectrochimica Acta Part A: Molecular and Biomolecular Spectroscopy* 137 (2015) 1126-1143.